19th Australasian Fluid Mechanics Conference
Melbourne, Australia
8-11 December 2014

Linear Stability of Natural Convection Induced by Absorption of Radiation in a Parallelepiped Cavity

A. Naghib, T. Hattori, J.C. Patterson and C. Lei

School of Civil Engineering

The University of Sydney, Sydney, NSW 2006, Australia

Abstract

This study focuses on the marginal stability of internally heated natural convection flow due to the absorption of incoming radiation in a parallelepiped cavity. The study is motivated by possible limnological applications where natural convection is known to have a significant impact on transport and mixing phenomena. The absorption of incoming radiation by a water body follows Beer's law, and any residual radiation reaching the bottom is absorbed by the bottom and re-emitted as a boundary flux. A potentially unstable bottom thermal boundary layer forms below a layer of stable thermal stratification, which exponentially decays from the water surface. The thermal structures evolve with time, and hence the pattern formation and critical conditions of the convective instability vary with time. A frozen-time model is employed in the present study and the base flow solution is assumed to be quasi-static for the evolution of perturbation. Despite a large body of literature available for the classical Rayleigh-Benard convection, the stability analysis on internally heated convection within a confined domain is very limited. The purpose of the present study is to investigate the dependence of three-dimensional pattern formation and critical conditions on the aspect ratio of the cavity and the water depth, and their time evolutions.

Introduction

Understanding mixing and transport mechanisms helps monitor water quality changes in water resources. Thermal forcing is one of the main driving factors that promotes mixing and plays an important role on changes in water quality within water bodies, such as lakes and reservoirs. Adams & Wells [1], Monismith et al. [2], and Macintyre & Melack [3] have shown that induced natural convection significantly impacts the water quality of the aforementioned water resources.

The present study focuses on the natural convection induced by absorption of solar radiation. During the day, solar radiation penetrates into water body and the intensity of the radiation decays due to absorption according to Beer's law:

$$I = I_0 \exp(-\eta h) \qquad (h \geq 0), \tag{1}$$

where h is water depth, η is a bulk attenuation coefficient of water and I_0 is the radiation intensity at the water surface (h=0). The absorption of incoming radiation produces a thermally stably stratified layer. Any residual radiation at the bottom is assumed to be absorbed by the bed and forms a bottom heat flux which is a potential source of Rayleigh-Benard type instability. Thus, there are two competing thermal layers: a stable surface layer due to the direct absorption of solar radiation and a potentially unstable bottom layer resulting from the residual heat flux at the bed. This leads to the formation of a nonlinear temperature profile, which, along with the free surface condition considered here, differentiates the present problem from the convectional Rayleigh-Benard problem.

Stability of this type of flow has been studied for an infinite horizontal fluid layer by Farrow and Patterson [4] and for a laterally confined fluid layer with horizontal through-flow by Hattori et. al. [5]. The aim of this study is to extend the previous studies to consider the effects of insulating sidewalls in a three dimensional domain.

The linear stability of the Rayleigh-Benard (RB) problem in a three-dimensional cavity has been studied extensively. Davis [6] investigated the stability of the fluid in a rectangular box heated from below for the case of conductive walls in 1967 while assuming two-dimensional finite rolls, in which the two nonzero velocity components depends on all three spatial variables. The critical Rayleigh number was obtained for different aspect ratios, and it was concluded that finite rolls with their axes perpendicular to a larger side are the preferred mode of convection. Catton [7, 8] investigated the same problem, also assuming the formation of finite rolls, and pointed out that Davis violated Weierstrass theorem in the Galerkin method. Catton, however, confirmed the above finding by Davis for both conductive and insulating sidewalls.

Mukutmoni & Yang [9] evaluated the critical Rayleigh number based on a three-dimensional numerical simulation of the flow in a cavity with insulating sidewalls. Mizushima & Matsuda [10] considered all three velocity components in their linear stability analysis and evaluated the critical Rayleigh number for the onset of instability in a cubic cavity with conductive sidewalls. Mizushima & Nakamura [11] evaluated the critical Rayleigh number for a parallelepiped cavity with insulating sidewalls in 2003 and obtained a three-dimensional disturbance patterns at the onset of instability.

The objectives of this paper are to evaluate the critical Rayleigh number for the onset of three-dimensional instability induced by the absorption of solar radiation in a parallelepiped cavity, to obtain disturbance patterns, and to investigate their dependencies on the aspect ratio of the cavity, water depth and time.

Problem Formulation

The geometry of the problem is defined in figure 1. The co-ordinate origin is at the centroid of the parallelepiped cavity.

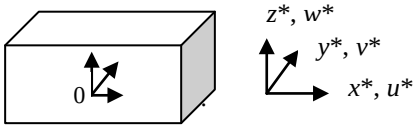

Figure 1. Parallelepiped cavity. The dimensions in the x and y directions are L_x and L_y, respectively while the dimension in the z direction is h.

Assuming constant water properties at ambient temperature with the Boussinesq approximation, the governing equations are written as follows:

$$\frac{\partial u^*}{\partial t^*}+u^*\frac{\partial u^*}{\partial x^*}+v^*\frac{\partial u^*}{\partial y^*}+w^*\frac{\partial u^*}{\partial z^*}=-\frac{1}{\rho_0}\frac{\partial p^*}{\partial x^*}+\upsilon\nabla^{*2}u^*,$$

$$\frac{\partial v^*}{\partial t^*}+u^*\frac{\partial v^*}{\partial x^*}+v^*\frac{\partial v^*}{\partial y^*}+w^*\frac{\partial v^*}{\partial z^*}=-\frac{1}{\rho_0}\frac{\partial p^*}{\partial y^*}+\upsilon\nabla^{*2}v^*,$$

$$\frac{\partial w^*}{\partial t^*}+u^*\frac{\partial w^*}{\partial x^*}+v^*\frac{\partial w^*}{\partial y^*}+w^*\frac{\partial w^*}{\partial z^*}=-\frac{1}{\rho_0}\frac{\partial p^*}{\partial z^*}+\upsilon\nabla^{*2}w^*+g\gamma(T^*-T_0^*), \quad (2)$$

$$\frac{\partial T^*}{\partial t^*}+u^*\frac{\partial T^*}{\partial x^*}+v^*\frac{\partial T^*}{\partial y^*}+w^*\frac{\partial T^*}{\partial z^*}=\kappa\nabla^{*2}T^*+\frac{I_0}{\rho_0 C_p}\eta\exp(\eta(z^*-0.5h)),$$

$$\frac{\partial u^*}{\partial x^*}+\frac{\partial v^*}{\partial y^*}+\frac{\partial w^*}{\partial z^*}=0,$$

where u^*, v^* and w^* are the velocity components in x, y and z directions respectively; T^* is the temperature; p^* is the pressure; ∇^{*2} is the Laplacian operator. The density, kinematic viscosity, thermal diffusivity, gravitational acceleration and thermal expansion coefficient are ρ_0, υ, κ, g, γ, respectively. The source term in the energy equation represents the direct absorption of solar radiation according to Beer's law.

The boundary conditions on the sidewalls are expressed as:

$$u^*=v^*=w^*=\frac{\partial T^*}{\partial x^*}=0 \quad (x^*=\pm\frac{L_x}{2}),$$
$$u^*=v^*=w^*=\frac{\partial T^*}{\partial y^*}=0 \quad (y^*=\pm\frac{L_y}{2}). \quad (3)$$

The top boundary is a stress-free surface and is assumed to be insulating:

$$\frac{\partial u^*}{\partial z^*}=\frac{\partial v^*}{\partial z^*}=w^*=\frac{\partial T^*}{\partial z^*}=0 \quad (z^*=0.5h). \quad (4)$$

The bottom boundary is a rigid wall, and the residual radiation at the bottom is assumed to be absorbed and re-emitted as a boundary heat flux, the following boundary conditions are applied at the bottom [4]:

$$u^*=v^*=w^*=0,$$
$$\frac{\partial T^*}{\partial z^*}=-\frac{I_0}{\rho_0 C_p\kappa}exp(-\eta h) \quad (z^*=-0.5h). \quad (5)$$

Normalization is carried out using the following scales: the length scales are L_x, L_y, and η^{-1} in the x, y and z direction, respectively; the velocity scales are κ/L_x, κ/L_y and $\kappa\eta$ in the x, y, and z direction, respectively; the time scale is $(\kappa\eta^2)^{-1}$; the temperature scale is $I_0/(\rho_0 C_p\kappa\eta)$; and the pressure scale is $\gamma g I_0/(C_p\kappa\eta^2)$. The Laplacian operator is normalized by η^2, hence, the dimensionless Laplacian operator is written as:

$$\Delta=\nabla^2=\frac{1}{\alpha^2}\frac{\partial^2}{\partial x^2}+\frac{1}{\beta^2}\frac{\partial^2}{\partial y^2}+\frac{\partial^2}{\partial z^2}, \quad (6)$$

where $\alpha = L_x\eta$ and $\beta = L_y\eta$. Ra and Pr are the Rayleigh number and the Prandtl number, defined respectively as:

$$Ra=\frac{g\gamma I_0}{\rho_0 C_p\upsilon\kappa^2\eta^4},$$
$$Pr=\frac{\upsilon}{\kappa}. \quad (7)$$

In order to simplify the numerical calculation, the solenoidal velocity field $\bar{u}$ is introduced using two scalar functions ψ^{1*} and ψ^{2*} [12]:

$$\vec{u}^*=\nabla^*\times\psi^{1*}\vec{i}+\nabla^*\times\psi^{2*}\vec{j}, \quad (8)$$

where $\vec{i}$ and $\vec{j}$ are the unit vectors in the x and y directions respectively.

The base flow is governed by a one-dimensional conduction equation, and the base temperature is given as [4]:

$$\bar{T}(z,t)=\frac{t}{h\eta}-\exp(z-0.5h\eta)+\frac{(z-0.5h\eta)^2}{2h\eta}+z-0.5h\eta+\frac{1}{3}h\eta+\frac{1}{h\eta}(1-\exp(-h\eta))-\frac{2}{h\eta}\sum_{n=1}^{\infty}\left[\frac{1}{(n\pi/h\eta)^2}-\frac{1-(-1)^n\exp(-h\eta)}{1+(n\pi/h\eta)^2}\right]\exp\left(-\left(\frac{n\pi}{h\eta}\right)^2 t\right)\cos\left(\frac{n\pi}{h\eta}(z-0.5h\eta)\right), \quad (9)$$

where the value of the normalized water depth (ηh) determines the relative strength of a stable surface layer over a potentially unstable bottom layer. For shallow water depth (ηh<1), the penetration depth of solar radiation is greater than the water depth, which results in the formation of potentially unstable thermal layer across the full depth. On the other hand, for a deep water depth (ηh>1), a substantial amount of the radiation is directly absorbed by the water body, which leads to the formation of a stably stratified surface layer [4, 5].

Based on the frozen-time assumption, the perturbation components are expanded as follows:

$$\psi^1(x,y,z,t)=\psi^1(x,y,z)exp(St),$$
$$\psi^2(x,y,z,t)=\psi^2(x,y,z)exp(St), \quad (10)$$
$$\theta(x,y,z,t)=\theta(x,y,z)exp(St),$$

where S is the growth rate of the perturbation and θ is the temperature perturbation. Consequently, the linearised perturbation equations are obtained as:

$$\left[(\frac{\partial^2}{\partial z^2}+\frac{1}{\beta^2}\frac{\partial^2}{\partial y^2})\Delta\psi^1-\frac{1}{\alpha^2}\frac{\partial^2}{\partial x\partial y}(\Delta\psi^2)\right]-Ra\frac{\partial\theta}{\partial y}=+\frac{S}{Pr}(\frac{1}{\beta^2}\frac{\partial^2\psi^1}{\partial y^2}+\frac{\partial^2\psi^1}{\partial z^2}-\frac{1}{\alpha^2}\frac{\partial^2\psi^2}{\partial x\partial y}),$$
$$\left[-(\frac{\partial^2}{\partial z^2}+\frac{1}{\alpha^2}\frac{\partial^2}{\partial x^2})\Delta\psi^2+\frac{1}{\beta^2}\frac{\partial^2}{\partial x\partial y}(\Delta\psi^1)\right]-Ra\frac{\partial\theta}{\partial x}=-\frac{S}{Pr}(\frac{1}{\alpha^2}\frac{\partial^2\psi^2}{\partial x^2}+\frac{\partial^2\psi^2}{\partial z^2}-\frac{1}{\beta^2}\frac{\partial^2\psi^1}{\partial x\partial y}), \quad (11)$$
$$\Delta\theta+(\frac{1}{\beta^2}\frac{\partial\psi^1}{\partial y}-\frac{1}{\alpha^2}\frac{\partial\psi^2}{\partial x})\times\frac{\partial\bar{T}}{\partial z}=S\theta.$$

The boundary conditions for the perturbation components are:

$$\begin{aligned}
&\psi^1 = \psi^2 = \frac{\partial \psi^2}{\partial x} = \frac{\partial \theta}{\partial x} = 0 \qquad (x = \pm\frac{1}{2}),\\
&\psi^1 = \psi^2 = \frac{\partial \psi^1}{\partial y} = \frac{\partial \theta}{\partial y} = 0 \qquad (y = \pm\frac{1}{2}),\\
&\psi^1 = \psi^2 = \frac{\partial^2 \psi^1}{\partial z^2} = \frac{\partial^2 \psi^2}{\partial z^2} = \frac{\partial \theta}{\partial z} = 0 \qquad (z = +\frac{1}{2}h\eta),\\
&\psi^1 = \psi^2 = \frac{\partial\ \psi^1}{\partial z} = \frac{\partial\ \psi^2}{\partial z} = \frac{\partial \theta}{\partial z} = 0 \qquad (z = -\frac{1}{2}h\eta).
\end{aligned} \tag{12}$$

Equations (11) and (12) at S=0 (marginal stability) form an eigenvalue problem for Ra and the corresponding eigenfunctions, i.e., ψ^1, ψ^2, θ. It is clear that the critical value of Ra (Ra_c) is independent of the fluid type, specified by Pr, at the marginal stability; however, it depends on α, β, $h\eta$, and t. It is worth mentioning that the classical RB problem has a linear temperature profile and symmetrical boundary conditions, and therefore the Galerkin method is appropriate due to the simplicity of trial functions, which is not the case in the present study, as discussed in [5]. Hence, the finite difference method with a second-order discretisation scheme on a uniform mesh is employed. The critical Ra and eigenfunctions are obtained for given values of α, β, $h\eta$, and t.

Numerical Results

The perturbation equations (11) are the same as those for the conventional RB problem. In order to validate the computational code, the boundary conditions and the base temperature profile are modified for the RB convection in a cubic cavity with conductive sidewalls. The critical Rayleigh number for the onset of thermal convection is calculated for different mesh sizes. It has been confirmed that the critical Rayleigh number Ra_c converges to the value of 6798 reported in Mizushima and Matsuda (1997) using 25 computational nodes in each direction.

In the following we provide some preliminary results obtained using a relatively coarse mesh (25 computational nodes in each direction) in a square cavity. It should be noted that the number of the computational nodes is sufficient to resolve the bottom boundary layer for $t > 0.01$.

The effect of the aspect ratio on the critical Rayleigh number is illustrated in figure 2 for $h\eta$=1.0 and t=0.05. As the aspect ratios, α and β, increase, the value of the critical Rayleigh number reduces and converges to the value for a horizontally unconfined fluid layer, which is 1.26E+4 for the corresponding case [4]. The asymptotic convergence of the critical Rayleigh number with the increasing lateral extent has also been shown in [5]. As widely reported for conventional Rayleigh-Benard convection, e.g. [6], and also shown in [5], reducing the lateral extent of the flow domain stabilises the flow, therefore the critical Rayleigh number increases. The stabilising effect of the lateral confinement is explained in [6] as follows; decreasing the size of the box dissipates the potential energy due to an increase in viscous effects.

The three-dimensional results for t=0.01, α=β=2, and $h\eta$=1.25 are shown in figure 3. The cross section of the three-dimensional results is plotted in figure 4((d)-(f)).

As shown in figures 4 ((a)-(c)), 4 ((d)-(f)), and 5 ((a)-(c)) for $h\eta$=1.25 and t=0.01, with increasing α and β the number of rolls increases, which is consistent with [5], so that the number of growing plumes increases.

It is also evident from the results in figures 5((a)-(c)) and 5((d)-(f)) that for α=β=4.0 and t=0.01, the number of rolls reduces as the values of $h\eta$ decreases, which is again consistent with the results of the previous studies [4, 5].

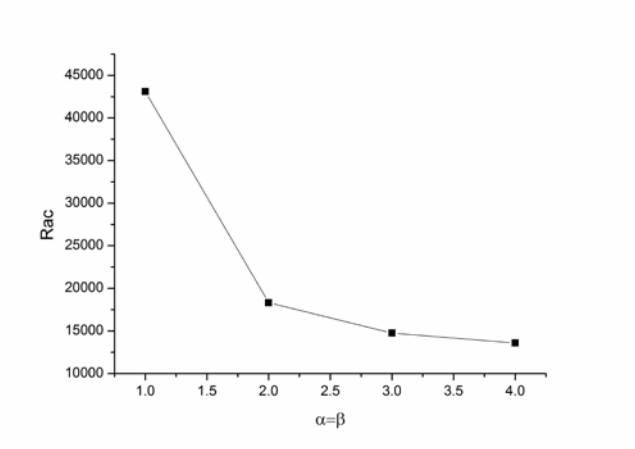

Figure 2. The critical Rayleigh number versus different value for α and β at $h\eta$=1.0 and t=0.05

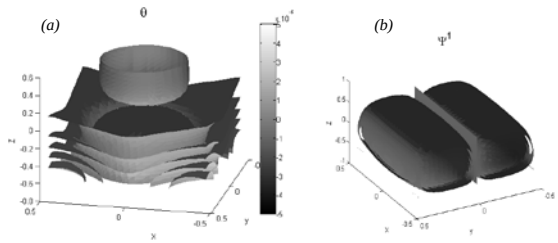

Figure 3. Three-dimensional pattern of ψ^1, and θ at the critical point (Ra=Ra_c), t=0.01, α=β=2.0, and $h\eta$=1.25

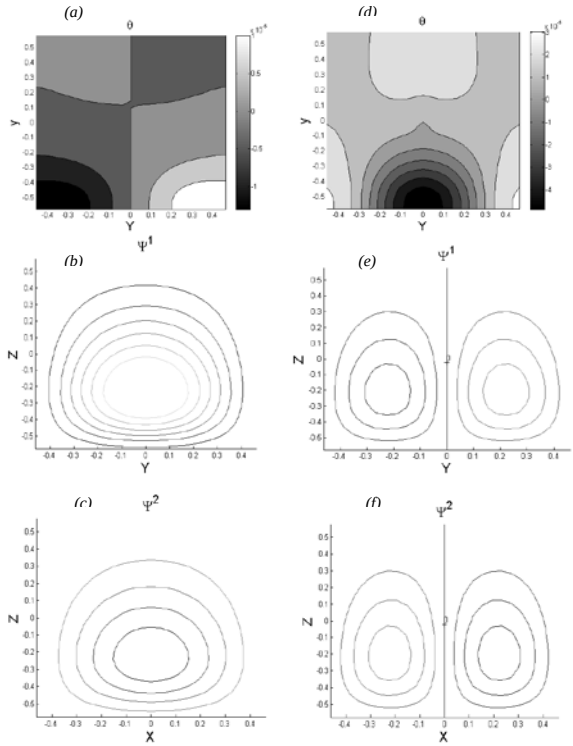

Figure 4. Isocontours of ψ^1(at x=0), ψ^2 (at y=0) and θ (at x=0) at the critical state (Ra=Rac), $h\eta$=1.25 and t=0.01: i) α=β=1.0 ((a)-(c)); ii) α=β=2.0 ((d)-(f))

Comparing the results shown in figure 5((a)-(c)) and figure 6((a)-(c)), for α=β=4.0 and $h\eta$=1.25 at two different times, it is clear that the number of rolls reduces as time increases, which

confirms the results of the previous studies [4, 5]. As time increases, the bottom thermal boundary layer grows and as a consequence, the temperature pattern shown in figure 6*(a)* extends further compared to the pattern shown in figure 5*(a)*.

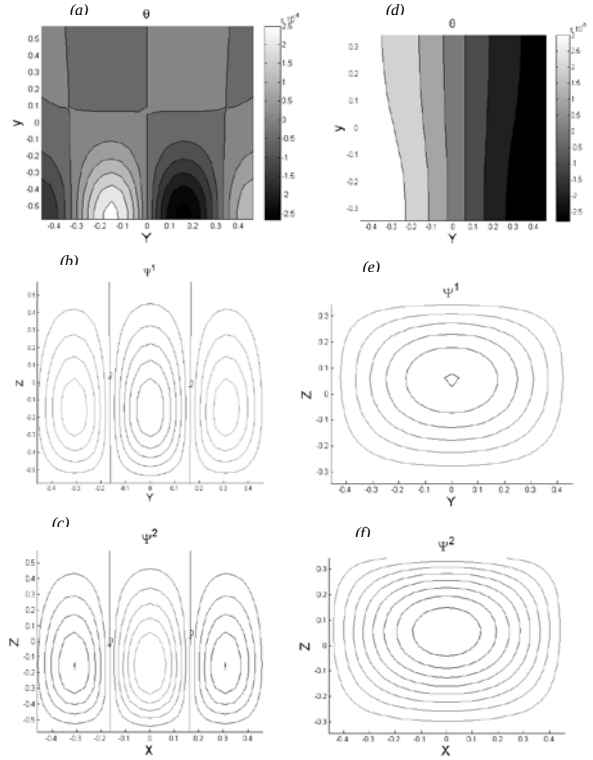

Figure 5. Isocontours of ψ^1(at x=0), ψ^2 (at y=0) and θ (at x=0) at the critical point (Ra=Rac), t=0.01 and α=β=4.0: *i*) $h\eta$=1.25 (*(a)-(c)*) *; ii*) $h\eta$=0.75 (*(d)-(f)*)

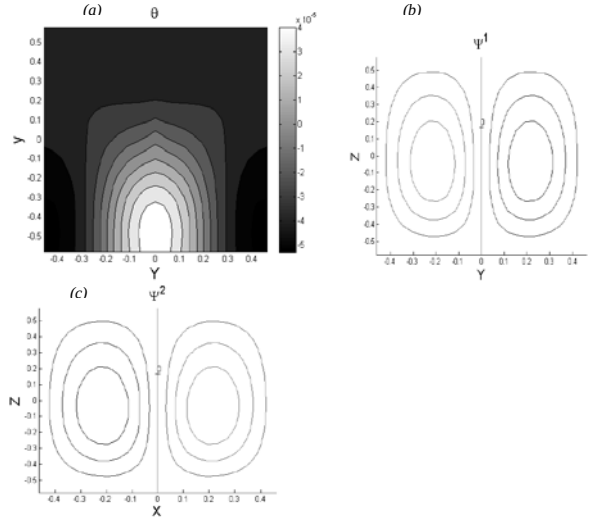

Figure 6. Isocontours of ψ^1(at x=0), ψ^2 (at y=0) and θ (at x=0) at the critical point (Ra=Rac), t=0.05, α=β=4.0, and $h\eta$=1.25

Conclusion

The aim of this paper is to investigate the marginal stability of convection induced by solar radiation in a parallelepiped cavity with insulating sidewalls. All the three velocity components are taken into account in the perturbation equations.

The results showed that at a fixed $h\eta$ and t, as the aspect ratio (α and β) increases, the fluid is destabilised and therefore Ra_c reduces. In addition, the increase of α and β results in an increasing number of rolls, which corresponds to an increase in the number of observed plumes. Further, by decreasing $h\eta$ while keeping the other parameters (α, β, t) constant, the number of rolls reduces. It is also evident that for a fixed set of α, β, and $h\eta$, the number of rolls reduces with time. The future study will focus on the impact of unequal aspect ratios on critical conditions, three-dimensional pattern formation, and their time evolutions for various water depths in a parallelepiped cavity.

Acknowledgement

This research is financially supported by the Australian Research Council.

References

[1] Adams, E.E. & Wells, S.A., Field Measurements on Side Arms of Lake Anna, VA, *J. Hydraul. Eng.*,**110**, 1984**,** 773–793.

[2] Monismith, S.G., Imberger, J. & Morison, M.L., Convective Motions in the Sidearm of a Small Reservoir, *Limnol. Oceanogr.*,**35**, 1990**,** 1676–1702.

[3] Macintyre, S. & Melack, J.M., Vertical and Horizontal Transport in Lakes Linking Littoral, Benthic, and Pelagic Habitats, *J. North Am. Benthol. Soc.*,**14**, 1995**,** 599-615.

[4] Farrow, D.E. & Patterson, J.C., On the Stability of the Near Shore Waters of a Lake When Subject to Solar Heating, *Int. J. Heat Mass Transf.*,**36**, 1993, 89–100.

[5] Hattori, T., Patterson, J.C. & Lei, C., On the Stability of Internally Heated Natural Convection due to the Absorption of Radiation in a Laterally Confined Fluid Layer with a Horizontal Throughflow, *(Unpublished).*

[6] Davis, S.H., Convection in a Box : Linear Theory, *J. Fluid Mech.*,**30**, 1967**,** 465–478.

[7] Catton, I., Convection in a Closed Rectangular Region the Onset of Motion, *Trans. ASME*,**92**, 1970**,** 186–188.

[8] Catton, I., The Effect of Insulating Vertical Walls on the Onset of Motion in a Fluid Heated from Below, *Int. J. Heat Mass Transf.*,**15**, 1972**,** 665–672.

[9] Mukutmoni, D. & Yang, K.T., Thermal Convection in Small Enclosures: an Atypical Bifurcation Sequence, *Int. J. Heat Mass Transf.*,**38**, 1995, 113–126.

[10] Mizushima, J. & Matsuda, O., Onset of 3D Thermal Convection in a Cubic Cavity, *J. Phys. Soc. Japan*,**66**, 1997**,** 2337–2341.

[11] Mizushima, J. & Nakamura, T., Onset of Three-Dimensional Thermal Convection in a Rectangular Parallelepiped Cavity, *J. Phys. Soc. Japan*,**72**, 2003**,** 197–200.

[12] Kessler, R., Nonlinear Transition in Three-dimensional Convection, *J. Fluid Mech.*,**174**, 1987, 357–379.